

# ***In vivo* fiber-optic confocal reflectance microscope with an injection-molded plastic miniature objective lens**

Kristen Carlson, Matthew Chidley, Kung-Bin Sung, Michael Descour, Ann Gillenwater, Michele Follen, and Rebecca Richards-Kortum

For *in vivo* optical diagnostic technologies to be distributed to the developed and developing worlds, optical imaging systems must be constructed of inexpensive components. We present a fiber-optic confocal reflectance microscope with a cost-effective injection-molded plastic miniature objective lens for *in vivo* imaging of human tissues in near real time. The measured lateral resolution is less than 2.2  $\mu\text{m}$ , and the measured axial resolution is 10  $\mu\text{m}$ . Confocal images of *ex vivo* cervical tissue biopsies and *in vivo* human lip taken at 15 frames/s demonstrate the microscope's capability of imaging cell morphology and tissue architecture. © 2005 Optical Society of America

OCIS codes: 170.1610, 170.1790, 170.2150, 170.3880, 170.4440, 170.4730.

## **1. Introduction**

Cancer is a significant public health problem worldwide. Annually, over 6 million people die from cancer, and over 10 million new cancer cases are detected.<sup>1</sup> The incidence and mortality of many cancers (e.g., cervical cancer) have been reduced through the use of screening programs to detect treatable precancerous lesions. However, many developing countries do not have adequate resources to implement currently available screening programs. For example, India has a high incidence of oral and cervical cancers, approximately 50,000 and 125,000 new cases per year, respectively.<sup>2</sup> Both of these cancers are preventable if detected in the earliest stages of development, yet nearly 30,000 oral and 70,000 cervical cancer patients die each year in India. The current method of cancer and precancer detection in these organ sites requires tissue removal and *in vitro* analysis of cel-

lular and nuclear morphologic features of tissue sections. Techniques to obtain this information noninvasively, *in vivo*, and in real time have the potential of decreasing the costs associated with cancer screening programs.<sup>3</sup> *In vitro* studies have shown the capability of confocal reflectance microscopy to provide this same morphological information noninvasively and in real time by use of the principle of optical sectioning.<sup>4</sup>

Confocal reflectance microscopy is an imaging technology that acquires backscattered light from small volumes within a sample to construct images with microscopic resolution at depths up to several hundred micrometers. Confocal imaging of tissue can provide histologic-quality images of cell morphology and tissue architecture in real time. *In vivo* confocal reflectance microscopy was first applied to the more accessible organs, such as the eye,<sup>5</sup> the skin,<sup>6</sup> and the lip.<sup>7</sup> Many imaging sites of interest, such as the uterine cervix and the oral cavity, require flexible fiber-based microscopes with miniature objective optics. Several groups have investigated configurations of fiber-based endoscopes by using either a single fiber<sup>8–10</sup> or a fiber bundle<sup>11–13</sup> for fluorescence or reflectance confocal imaging. *In vivo* images have been obtained by use of confocal fluorescence endoscopes with fluorescent dyes.<sup>12,14,15</sup> However, fluorescent dyes used *in vivo* must be nontoxic and capable of penetrating deeply into the tissue. Reflectance imaging uses native index-of-refraction variations as a source of contrast. In epithelial tissue, acetic acid can

---

K. Carlson (kristencarlson@mail.utexas.edu), K.-B. Sung, and R. Richards-Kortum are with the Department of Biomedical Engineering, The University of Texas at Austin, 1 University Station, C0800 ENS10, Austin, Texas 78712. M. Childley and M. Descour are with the Optical Sciences Center, The University of Arizona, Tucson, Arizona 86721. A. Gillenwater and M. Follen are with the M. D. Anderson Cancer Center, The University of Texas, Houston, Texas 77030.

Received 20 July 2004; revised manuscript received 23 November 2004; accepted 23 November 2004.

0003-6935/05/101792-06\$15.00/0

© 2005 Optical Society of America

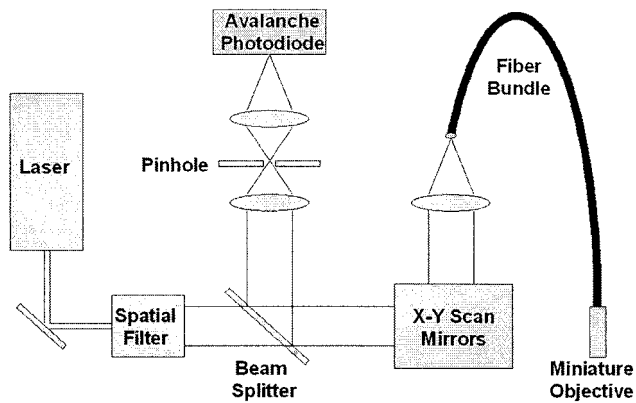


Fig. 1. Schematic of fiber-optic confocal reflectance microscope (FOCM).

be applied to enhance the contrast between nuclei and the surrounding cytoplasm.<sup>16</sup> *In vivo* imaging using confocal reflectance endoscopes has few reported results, owing to low signal and contrast levels. Use of high-numerical-aperture optics, sensitive detectors, and acetic acid for improved contrast have compensated for these obstacles, and the viability of confocal reflectance microscopy has been demonstrated *in vivo*.<sup>17</sup>

We previously presented a fiber bundle confocal reflectance microscope for *in vivo* imaging.<sup>13,18</sup> A glass miniature objective lens was designed and used to enable *in vivo* imaging of the cervix and oral cavity.<sup>17,19</sup> These glass objective lenses provide high-resolution *in vivo* imaging; however, they are difficult to produce, and assemble and manufacturing costs are extremely high (approximately \$8000 per objective). For this valuable imaging technology to be tested in multicenter trials and potentially distributed to clinics in developed and developing worlds, more cost-effective and manufacturable solutions must be explored. Injection-molded plastic miniature objective lenses could potentially provide an inexpensive substitute for these costly glass lenses. The actual cost for injection molding and antireflection coating one objective lens used to obtain images presented in this paper was \$350 in a prototype run of 50 objectives. A reasonable production run estimate for these injection-molded plastic objective lenses is \$50 per objective. In this paper we present imaging results for our fiber-optic confocal microscope with an inexpensive injection-molded plastic miniature objective lens.

## 2. Materials and Methods

### A. Fiber-Optic Confocal Microscope

Figure 1 shows a schematic of the *in vivo* fiber-optic confocal reflectance microscope (FOCM). Details and performance of the system were presented previously.<sup>18,19</sup> Briefly, this system uses a coherent fiber bundle image guide with 30,000 fibers, an outer diameter of 2.5 mm, and a nominal numerical aperture of 0.3.

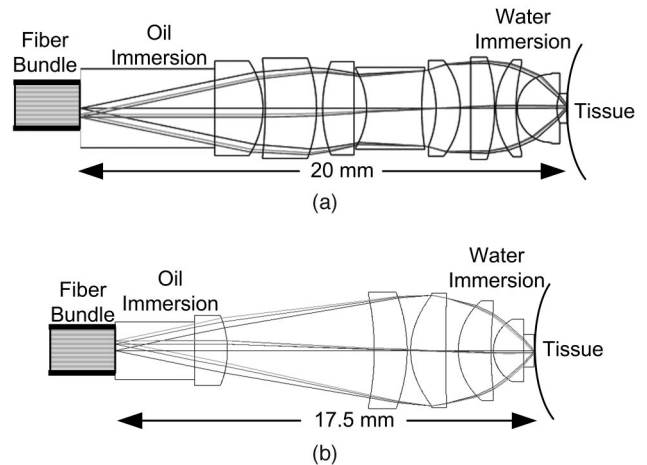


Fig. 2. Optical design of miniature objective lenses used in FOCM. Here the fiber bundle is located to the left of the lenses, with oil immersion. The sample is placed to the right, with water immersion. (a) Previous glass lens design with eight lens elements. (b) New plastic lens design with five lens elements utilizing aspheric surfaces.

Each fiber is approximately 4  $\mu\text{m}$  in diameter with 7  $\mu\text{m}$  center-to-center spacing between fibers. Index-matching oil is used at both fiber bundle surfaces to suppress specular reflection, and 1064-nm light is raster scanned horizontally by a resonant mirror and vertically by a galvanometer mirror across the fiber bundle at a rate that generates images at 15 frames/s. Here we replace the glass miniature objective lens used previously by an injection-molded plastic miniature objective lens. The complex miniature objective images the fiber onto the sample and collects light reflected from the sample. The light reflected from the tissue is refocused back into the fiber, passes back through the system, and is directed to an avalanche photodiode through a 20- $\mu\text{m}$  diameter pinhole. This pinhole is placed in a position conjugate to the illumination–detection fiber, allowing the system to detect light from a single fiber at a time.

### B. Injection-Molded Plastic Miniature Objective Lens

We have designed and manufactured a high-numerical-aperture miniature injection-molded plastic objective lens to replace the expensive glass objective lens in our FOCM.<sup>20,21</sup> In comparison with the eight spherical glass lenses in the current miniature objective lens [as seen in Fig. 2(a)], the new complex lens is composed of five injection-molded plastic lenses [Fig. 2(b)]. This reduction in the number of lenses is a result of the capability of incorporating aspheric surfaces in the injection-molding process, which is extremely difficult and expensive for glass lenses of this size.

The design of the injection-molded objective was completed by means of the ZEMAX lens design software. The original designs were based on polystyrene; however, polystyrene is not designed for prolonged operation in a moisture-rich environment. Zeonex E48R, a cyclo-olefin polymer developed by



Fig. 3. Injection-molded plastic objective lens assembled and disassembled with U.S. coins.

Zeon Corporation for high-precision molding applications, was chosen for its low water absorption and low birefringence.<sup>20</sup>

The design specifications for the plastic objective lens are equivalent to those for the previous glass lens. The lens has a numerical aperture in the object space (tissue side) of 1.0 and is designed for water immersion. At the optical fiber bundle, the numerical aperture is 0.3 with oil immersion. The working distance is 450  $\mu\text{m}$  with a 250- $\mu\text{m}$  diameter field of view. The lens is designed for 1064-nm-wavelength light and is telecentric in both the object and the image spaces. The maximum clear aperture is 5 mm, and the outer diameter is 7 mm. The total length from object to image is 17.5 mm.

The 7-mm outer diameter of the lens includes a flange, which serves as a mechanical mounting fixture. Alignment is achieved by selecting the appropriately sized ball bearing, nominally 500  $\mu\text{m}$  diameter, to place in the circular V-shaped alignment groove between each lens. In total, a constructed objective lens contains the five injection-molded plastic lenses with alignment flanges; a black, nonoptical plastic spacer; optically absorbing apertures that are placed between each pair of lens elements; and the alignment ball bearings. Figure 3 shows an assembled objective lens, along with a set of individual lenses and a spacer.

Given that the magnification is 3.33 and the lateral resolution is limited by the 7- $\mu\text{m}$  separation between adjacent fibers, the lateral resolution can be calculated as  $7 \mu\text{m}/3.33 = 2.1 \mu\text{m}$ . Following the method of Gu *et al.* for calculation of axial resolution in fiber confocal systems, the axial resolution of the FOCM with the plastic objective lens is also calculated to be 2.1  $\mu\text{m}$ .<sup>22</sup>

### C. Samples Imaged

The performance of the plastic miniature objective in the fiber-optic microscope was characterized by use of U.S. Air Force resolution test target, reflective grating, and polystyrene microspheres. To determine the system's capability for imaging cellular detail in thick tissue samples, we imaged cervical biopsy specimens. After patients gave informed consent to participate in

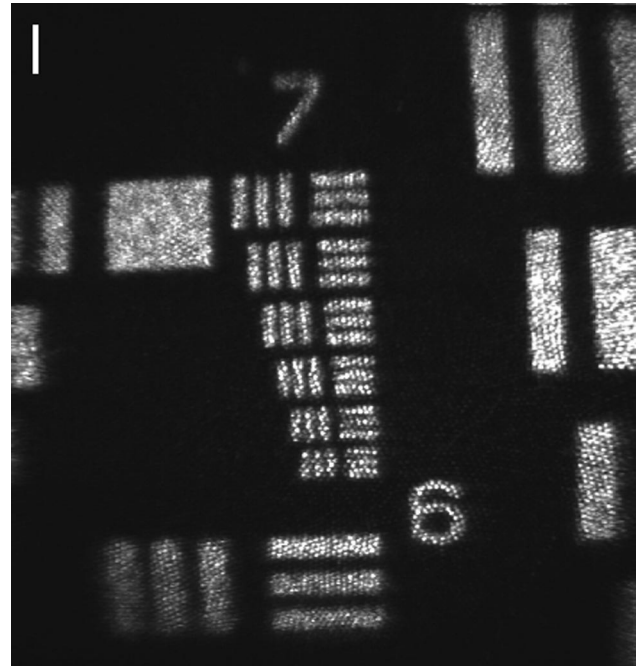


Fig. 4. Image of U.S. Air Force resolution test target demonstrating the lateral resolution of the plastic objective lens with the FOCM. The linewidths of the smallest element are 2.19  $\mu\text{m}$ . The scale bar is 20  $\mu\text{m}$ .

the study, biopsies were obtained during colposcopic examination at The University of Texas M. D. Anderson Cancer Center. Biopsies were treated with 6% acetic acid (vinegar) and fixed with 10% formaldehyde. During video acquisition, lateral movement and axial scanning were accomplished by moving the biopsy on a three-dimensional translation stage. *In vivo* images of the lower lip of a normal volunteer were obtained after application of 6% acetic acid. An electronic amplifier was used for the *in vivo* imaging to amplify the signal from the avalanche photodiode to provide brighter images on the monitor and instant feedback for the normal volunteer to facilitate sample positioning.

Background subtraction was applied to all images to reduce specular-reflection artifacts from the surface of the fiber bundle. In addition, images were resized in the horizontal direction to compensate for the nonlinearity of the resonant scanning mirror. The brightness and contrast of the presented *in vivo* image were adjusted to compensate for the amplified signal used in image acquisition.

### 3. Results

The lateral resolution of the FOCM was determined by imaging the seventh group on a U.S. Air Force resolution test target, as seen in Fig. 4. The line density for the elements in group 7 range from 128 to 228 line pairs/mm, corresponding to 3.91- and 2.19- $\mu\text{m}$  linewidths, respectively. The lines in the sixth element, which have linewidths of 2.19  $\mu\text{m}$ , can be resolved. Therefore the measured lateral resolution is less than 2.2  $\mu\text{m}$ , which is comparable with the

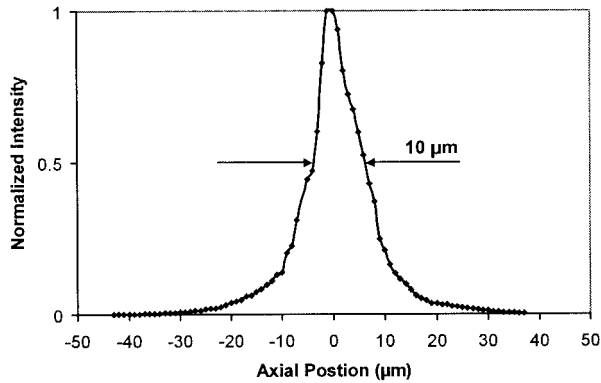


Fig. 5. Axial response of the FOCM with the plastic objective was measured by translation of a reflective grating through the focal plane of the objective in 1- $\mu\text{m}$  steps and acquisition of an image at each axial position. The bright region of the image was averaged for each image and plotted versus the axial position. The FWHM is approximately 10  $\mu\text{m}$ .

predicted value of 2.1  $\mu\text{m}$ . This method of measuring the lateral resolution was selected because the fiber pattern mask, seen in the images, can yield a misleading edge-response measurement.

The axial response of the confocal microscope was measured by scanning a reflective Ronchi grating through the focal plane of the system. Images were acquired in 1- $\mu\text{m}$  incremental steps. The gray values were averaged over a bright region in the center of the field of view for each image. Figure 5 shows the average intensity versus the axial position. The axial resolution is determined by measurement of the full width at half-maximum, which is measured to be approximately 10  $\mu\text{m}$ . The measured value is greater than the theoretical axial resolution; however, the optical sectioning capability is sufficient for imaging epithelial cell nuclei.

Figure 6 shows an image taken from a video of 4.3- $\mu\text{m}$  polystyrene microspheres imbedded in gelatin. Microspheres could be distinguished through a full scan of the 450- $\mu\text{m}$  working distance. The depth into the sample for the image in Fig. 6 is approximately 300  $\mu\text{m}$ . This image demonstrates the capability of the FOCM with a plastic objective to image objects of a size similar to that of epithelial cell nuclei.

A frame taken from a video of an axial scan through the epithelium of an *ex vivo* normal cervical biopsy is shown in Fig. 7. Nuclei could be detected throughout the epithelium, which was approximately 300  $\mu\text{m}$  in depth, based on the mechanical translation of the biopsy. The image plane of the image in Fig. 7 was located at approximately 200  $\mu\text{m}$  below the tissue surface. Similarly, a frame extracted from an *in vivo* video of the lower lip of a normal volunteer is shown in Fig. 8. The depth of the image plane in Fig. 8 is unknown but is approximately 50  $\mu\text{m}$  below the tissue surface. Nuclei can be seen clearly in *ex vivo* and *in vivo* videos and images, demonstrating the exceptional optical quality of the injection-molded plastic objective.

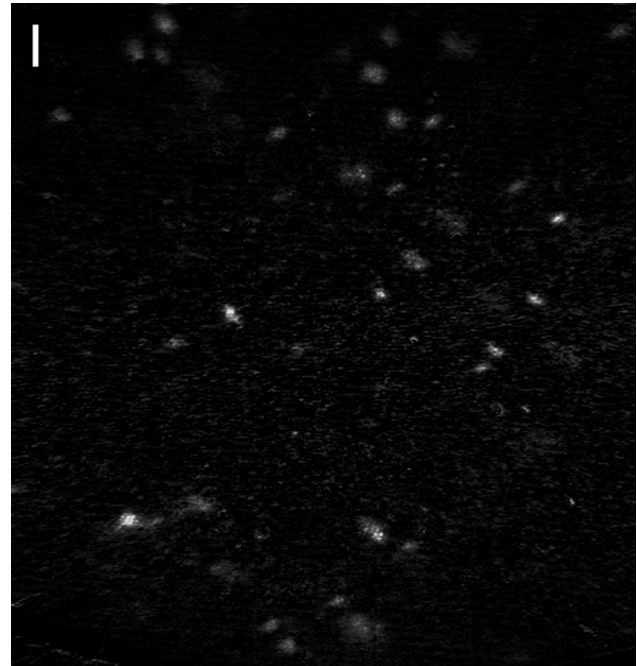


Fig. 6. Image of 4.3- $\mu\text{m}$  polystyrene microspheres imbedded in gelatin. The scale bar is 20  $\mu\text{m}$ .

#### 4. Discussion

These images demonstrate the imaging capability of the FOCM that uses an injection-molded plastic miniature objective lens. Videos acquired and displayed at 15 frames/s provide improved visualization of image detail compared with still images. Small movements of low-contrast objects in the videos aid the

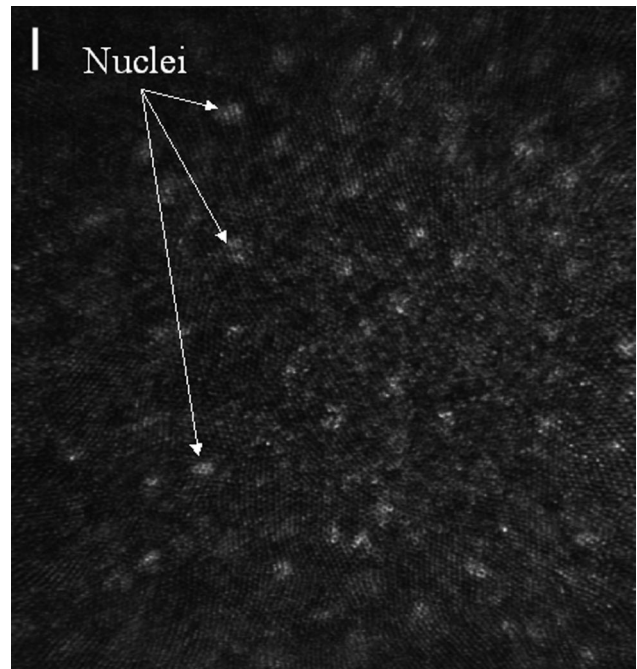


Fig. 7. Image of the epithelium of a normal cervical biopsy. The image plane is approximately 200  $\mu\text{m}$  below the surface. The scale bar is 20  $\mu\text{m}$ .

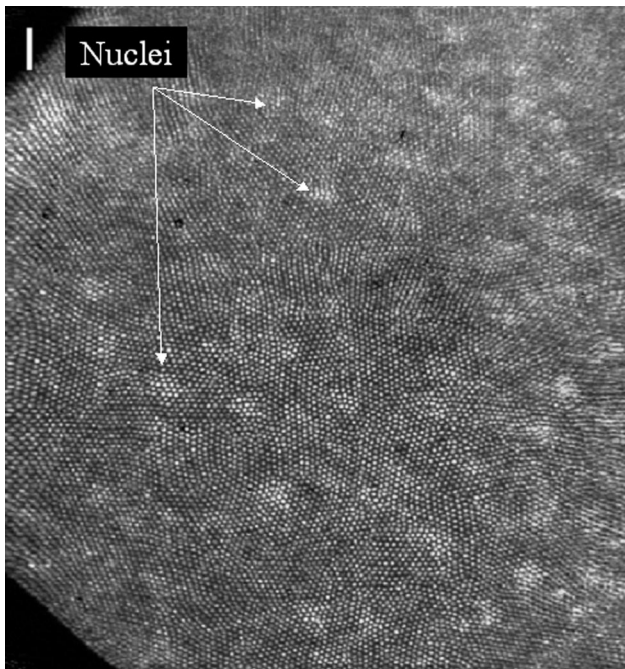


Fig. 8. Image of epithelium of the lower lip of a normal volunteer. The scale bar is 20  $\mu\text{m}$ .

viewer in discerning image features. Observing videos allows a visual time-averaging effect, reducing the pixilated appearance that results from the fiber bundle pattern.

The images presented here were acquired by use of a plastic objective lens mounted on an optical bench and connected to the FOCM via the fiber bundle. We plan to integrate the plastic objective lens into a handheld imaging probe, which would include the fiber bundle and an axial scanning mechanism. The plastic objective currently includes a groove in the outer perimeter of the lens closest to the tissue in order to provide water to the lens-tissue interface to suppress specular reflection. This groove will also be used in the future to facilitate axial scanning with hydraulic suction. The lens is designed such that the surface of the tissue is in the object plane of the objective lens when the rim of the lens is placed against the tissue. Axial scanning is accomplished by extracting water from the gap between the lens and the tissue, generating suction to move the tissue along the optical axis. This configuration also serves to stabilize the tissue to reduce motion artifacts during imaging. In future lens designs, the hydraulic channels could be directly incorporated into the assembled objective lens through the flange region of the individual lenses.

Once the plastic objective lens is integrated into a handheld probe, the FOCM will be completely situated on a portable cart for easy transfer to and from the clinic. During tissue examination, an operator controls the microscope from a computer. The probe is passed to the clinician to be placed on the tissue of interest. Images and videos are recorded for analysis

and comparison with histologic images of biopsies taken from the same sites.

## 5. Conclusion

We have presented a fiber-optic confocal reflectance microscope (FOCM) with an inexpensive injection-molded plastic objective lens for *in vivo* imaging of human tissues. The system and new cost-effective objective lens show sufficient lateral and axial resolution and sensitivity to image biological samples with subcellular resolution in near real time. This microscope will be used in clinical trials to determine the efficacy of confocal microscopy to detect dysplasia in cervical and oral cavity tissues *in vivo*. We anticipate that this emerging technology will ultimately make a significant contribution to the detection, monitoring, and therapy of precancers and cancers in epithelial tissues.

Financial support from the National Institutes of Health is gratefully acknowledged (grant R01-CA82880).

## References

1. World Health Organization, *National Cancer Control Programmes Policies and Managerial Guidelines*, 2nd. ed. (World Health Organization, Geneva, 2002); available at <http://www.who.int/cancer/media/en/408.pdf>.
2. J. Ferlay, F. Bray, P. Pisani, and D. M. Parkin, *Globocan 2000: Cancer Incidence, Mortality and Prevalence Worldwide* (World Health Organization International Agency for Research on Cancer, Lyon, 2001).
3. S. B. Cantor, M. F. Mitchell, G. Tortolero-Luna, C. S. Bratka, D. C. Bodurka, and R. Richards-Kortum, "Cost-effectiveness analysis of diagnosis and management of cervical squamous intraepithelial lesions," *Obstet. Gynecol.* **91**, 270–277 (1998).
4. T. Collier, A. Lacy, R. Richards-Kortum, A. Malpica, and M. Follen, "Near real-time confocal microscopy of amelanotic tissue: detection of dysplasia in *ex vivo* cervical tissue," *Acad. Radiol.* **9**, 504–512 (2002).
5. H. D. Cavanagh, J. V. Jester, J. Essepian, W. Shields, and M. A. Lemp, "Confocal microscopy of the living eye," *CLAO J.* **16**, 65–73 (1990).
6. M. Rajadhyaksha, M. Grossman, D. Esterowitz, R. H. Webb, and R. R. Anderson, "*In vivo* confocal scanning laser microscopy of human skin: melanin provides strong contrast," *J. Invest. Dermatol.* **104**, 946–952 (1995).
7. M. Rajadhyaksha, R. R. Anderson, and R. H. Webb, "Video-rate confocal scanning laser microscope for imaging human tissues *in vivo*," *Appl. Opt.* **38**, 2105–2115 (1999).
8. D. L. Dickensheets and G. S. Kino, "Silicon-micromachined scanning confocal optical microscope," *J. Microelectromech. Syst.* **7**, 38–47 (1996).
9. T. D. Wang, C. H. Contag, M. J. Mandella, N. Y. Chan, and G. S. Kino, "Dual-axes confocal microscopy with post-objective scanning and low-coherence heterodyne detection," *Opt. Lett.* **28**, 1915–1917 (2003).
10. G. J. Tearney, R. H. Webb, and B. E. Bouma, "Spectrally encoded confocal microscopy," *Opt. Lett.* **23**, 1152–1154 (1998).
11. A. F. Gmitro and D. Aziz, "Confocal microscopy through a fiber-optic imaging bundle," *Opt. Lett.* **18**, 565–567 (1993).
12. W. McLaren, J. Tan, and M. Quinn, "Detection of cervical neoplasia using non-invasive fibre-optic confocal microscopy," in *Proceedings of 5th International Multidisciplinary Congress*

- EUROGIN 2003*, J. Monsonogo, ed. (Monduzzi Editore, Paris, 2003), pp. 213–217.
13. K. B. Sung, C. Liang, M. Descour, T. Collier, M. Follen, and R. Richards-Kortum, "Fiber-optic confocal reflectance microscope with miniature objective for *in vivo* imaging of human tissues," *IEEE Trans. Biomed. Eng.* **49**, 1168–1172 (2002).
  14. Y. S. Sabharwal, A. R. Rouse, L. Donaldson, M. F. Hopkins, and A. F. Gmitro, "Slit-scanning confocal microendoscope for high-resolution *in vivo* imaging," *Appl. Opt.* **38**, 7133–7144 (1999).
  15. J. Knittel, L. Schnieder, G. Buess, B. Messerschmidt, and T. Possner, "Endoscope-compatible confocal microscope using a gradient index-lens system," *Opt. Commun.* **188**, 267–273 (2001).
  16. M. Rajadhyaksha, S. Gonzalez, and J. M. Zavislan, "Detectability of contrast agents for confocal reflectance imaging of skin and microcirculation," *J. Biomed. Opt.* **9**, 323–331 (2004).
  17. K. B. Sung, R. Richards-Kortum, M. Follen, A. Malpica, C. Liang, and M. Descour, "Fiber optic confocal reflectance microscopy: a new real-time technique to view nuclear morphology in cervical squamous epithelium *in vivo*," *Opt. Express* **11**, 3171–3181 (2003), <http://www.opticsexpress.org>.
  18. K. B. Sung, C. Liang, M. Descour, T. Collier, M. Follen, A. Malpica, and R. Richards-Kortum, "Near real time *in vivo* fibre optic confocal microscopy: sub-cellular structure resolved," *J. Microsc.* **207**, 137–145 (2002).
  19. C. Liang, K. B. Sung, R. R. Richards-Kortum, and M. R. Descour, "Design of a high-numerical-aperture miniature microscope objective for an endoscopic fiber confocal reflectance microscope," *Appl. Opt.* **41**, 4603–4610 (2002).
  20. M. D. Chidley, C. Liang, M. Descour, K. B. Sung, R. Richards-Kortum, and A. Gillenwater, "Miniature injection-molded optics for fiber-optic, *in vivo* confocal microscopy," in *International Optical Design Conference*, P. K. Manhart and J. M. Sasian, eds., *Proc. SPIE* **4832**, 126–136 (2002).
  21. M. D. Chidley and M. Descour, Optical Sciences Center, University of Arizona, 1630 E. University Boulevard, Tucson, Arizona 85721, are preparing a manuscript to be called "Design, assembly, and testing of high NA miniature injection-molded objective for laser confocal reflectance microscopy."
  22. M. Gu, C. J. R. Sheppard, and X. Gan, "Image formation in a fiber-optical confocal scanning microscope," *J. Opt. Soc. Am. A* **8**, 1755–1761 (1991).